

Rotationally Resolved Laser Photoelectron Spectra of Gas-Phase NO: Rotational Propensity Rules in Photoionization

K. S. Viswanathan, Ellen Sekreta, Ernest R. Davidson, and James P. Reilly*

Department of Chemistry, Indiana University, Bloomington, Indiana 47405 (Received: December 19, 1985)

Rotationally resolved laser photoelectron spectra were recorded by exciting specific rovibronic levels in the $A^2\Sigma^+$, $C^2\Pi$, and $D^2\Sigma^+$ Rydberg states of NO, to study the rotational propensity rules in photoionization. The data for the A and C states are in excellent agreement with theoretical calculations of Bonham et al. and the model of Pratt et al. The D state spectra show, in addition to the expected propensities, a strong $\Delta N = 0$ peak. On the basis of theoretical calculations we infer that the continuum wave excited by ionizing NO from its D state cannot be adequately described by a single l quantum number.

Introduction

For over a decade, the study of rotational propensity rules in molecular photoionization has been a subject of considerable interest.^{1,2} The first experiments to investigate these propensity rules were done by Åsbrink,¹ who recorded a rotationally resolved photoelectron spectrum, ionizing directly from the $1\Sigma_g^+$ ground state of H_2 to the $2\Sigma_g^+$ ground state of H_2^+ in a one-photon process. He observed a propensity rule of $\Delta N = 0, \pm 2$, as was predicted by Sichel.² (Here N is the quantum number that defines the total angular momentum, apart from spin, associated with the initial rotational level of H_2 and the final rotational level of H_2^+ .) Similar experiments were also performed by Morioka et al.³ and Pollard et al.⁴ confirming the results of Åsbrink. Single-photon photoelectron experiments of this type suffer from at least two limiting drawbacks. First, the resolution is barely adequate to clearly resolve rotational structure. This restricts the experiments to H_2 , which has a large rotational constant. Second, ionization takes place from a thermal distribution of rotational levels of the ground state and information about the rotational structure of the ions must be obtained through deconvolution.³

With the advent of the laser photoelectron technique,⁵⁻¹¹ the study of propensity rules has again received an impetus, since the best resolution (~ 3 meV) achieved with this technique is sufficient to clearly resolve rotational structure in at least a few lighter molecules. Furthermore, with this approach, one can excite specific rovibronic levels of different electronic states of the neutral in a first step and ionize from these levels in a subsequent step. This has three principal advantages. First, ionization takes place from selected rovibronic levels so simpler ion rotational state distributions are obtained than when ionizing from a thermal distribution of rotational levels. Second, relatively high J levels, for which the rotational energy spacing is large, can be selectively excited. Third, rotational propensity rules for ionization from different electronic states can be investigated. As a variation on the experiment done by Åsbrink, Pratt et al.⁹ ionized H_2 from its $B^1\Sigma_u^+$ state and observed the propensity rule of $\Delta N = \pm 1, \pm 3$, which differs from that found when photoionizing H_2 from its ground state. Theoretical calculations, in fact, show that the propensity rules depend not only on the symmetry of the two states involved in the photoionization process but also on the orbital angular momentum of the ejected electron.¹²

The purpose of the present work is to investigate the propensity rules for ionization from the $A^2\Sigma^+$, $C^2\Pi$, and $D^2\Sigma^+$ Rydberg states of NO. Nitric oxide was selected for this work, since many of its Rydberg states have been well studied and are easily reached by a one- or two-photon excitation.¹³⁻¹⁸ In an earlier paper¹⁹ we published a rotationally resolved spectrum obtained by ionizing NO from its $A^2\Sigma^+$ state. In that case, we observed a $\Delta N = 0, \pm 2$ propensity as had been predicted by Bonham and Lively.¹² Since then we have investigated the dependence of that spectrum on the laser polarization and have conducted similar experiments on the $C^2\Pi$ and $D^2\Sigma^+$ Rydberg states of NO. The latter two states

were two photon excited from the $X^2\Pi$ ground state of NO and then one photon ionized to the $X^1\Sigma^+$ ground state of NO^+ .

In their work on the photoionization of H_2 , Pratt et al.⁹ interpreted their rotationally resolved data by using a simple model based on the parities of the rotational levels. In arriving at the parities for the rotational levels of ion-electron complex, they used a case "d" coupling scheme since in the process of ionization the electron becomes loosely coupled to the ion core. It was assumed that the orbital angular momentum of the ejected electron changes by ± 1 unit (i.e., $\Delta l = \pm 1$). For example in their experiment on the B state of H_2 , in which a $2p\sigma$ electron was ejected, they assumed that only "s" and "d" continuum electron waves contribute to the process. Once the parities of the rotational levels of the ion-electron complex were worked out the rotational selection rules were obtained by requiring that in the course of photoionization parity must change and the change in the total angular momentum of the system, ΔJ , can be only 0 or ± 1 . This translated to a propensity rule of $\Delta N = \pm 1, \pm 3$ for ionization from the B state of H_2 , which they experimentally observed.

Using the same scheme, Dehmer arrived at a $\Delta N = 0, \pm 2$ propensity for ionization from the $3s\sigma A^2\Sigma^+$ state of NO,²⁰ which we investigated in our earlier experiments.¹⁹ This is depicted in Figure 1. An analogous scheme is shown in Figure 2 for ionization from the $3p\sigma D^2\Sigma^+$ state. In that case only s and d partial waves are assumed to contribute to the transition moment, and the propensities for transitions are expected to be $\Delta N = \pm 1, \pm 3$.

Figure 3 shows an analogous scheme for ionization from the $3p\pi C^2\Pi$ state. It can be seen that as long as Λ -doubling in the C state is not resolved the rotational propensity rules are expected to be $\Delta N = 0, \pm 1, \pm 2, \pm 3$. However, if Λ -doubling in the C state

- (1) Åsbrink, L. *Chem. Phys. Lett.* **1970**, *7*, 549.
- (2) Sichel, J. M. *Mol. Phys.* **1970**, *18*, 95.
- (3) Morioka, Y.; Hara, S.; Nakamura, M. *Phys. Rev. A* **1980**, *22*, 177.
- (4) Pollard, J. E.; Trevor, D. J.; Reutt, J. E.; Lee, Y. T.; Shirley, D. A. *J. Chem. Phys.* **1982**, *77*, 34 and references therein.
- (5) Meek, J. T.; Long, S. R.; Reilly, J. P. *J. Phys. Chem.* **1982**, *86*, 2809.
- (6) Anderson, S. L.; Rider, D. M.; Zare, R. N. *Chem. Phys. Lett.* **1982**, *93*, 11.
- (7) Achiba, Y.; Sato, K.; Kimura, K. *J. Chem. Phys.* **1983**, *78*, 5474.
- (8) Long, S. R.; Meek, J. T.; Reilly, J. P. *J. Chem. Phys.* **1983**, *79*, 3206.
- (9) Pratt, S. T.; Dehmer, P. M.; Dehmer, J. L. *J. Chem. Phys.* **1983**, *78*, 4315.
- (10) Miller, J. C.; Compton, R. N. *J. Chem. Phys.* **1981**, *75*, 22; *Chem. Phys. Lett.* **1982**, *93*, 453.
- (11) Kimman, J.; Kruit, P.; van der Wiel, M. J. *Chem. Phys. Lett.* **1982**, *88*, 576.
- (12) Bonham, R. A.; Lively, M. L. *Phys. Rev. A* **1984**, *29*, 1224.
- (13) Tanaka, Y. *J. Chem. Phys.* **1953**, *21*, 788.
- (14) Lagerqvist, A.; Miescher, E. *Helv. Phys. Acta* **1958**, *31*, 221.
- (15) Ackerman, F.; Miescher, E. *J. Mol. Spectrosc.* **1969**, *31*, 400.
- (16) Engleman, R.; Rouse, P. E. *J. Mol. Spectrosc.* **1971**, *37*, 240.
- (17) Asscher, M.; Haas, Y. *Chem. Phys. Lett.* **1978**, *59*, 231.
- (18) Sirkin, E. R.; Haas, Y. *Appl. Phys. Lett.* **1981**, *25*, 253.
- (19) Wilson, W. G.; Viswanathan, K. S.; Sekreta, E.; Reilly, J. P. *J. Phys. Chem.* **1984**, *88*, 672.
- (20) Dehmer, P. M., private communication, 1984.

* Alfred P. Sloan Fellow and Camille and Henry Dreyfus Teacher Scholar.

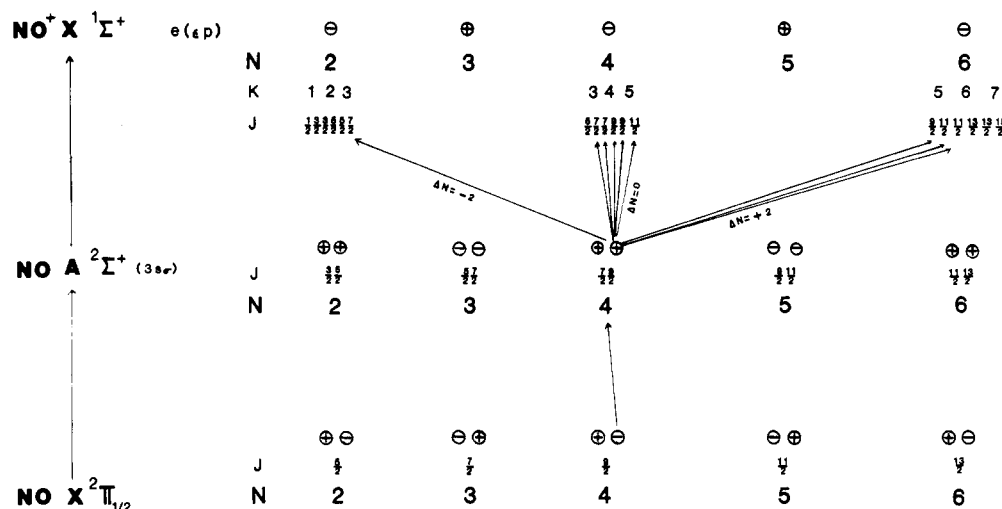


Figure 1. Allowed rotational transitions for a one-photon ionization from $J = 9/2$ of the A state.²⁰

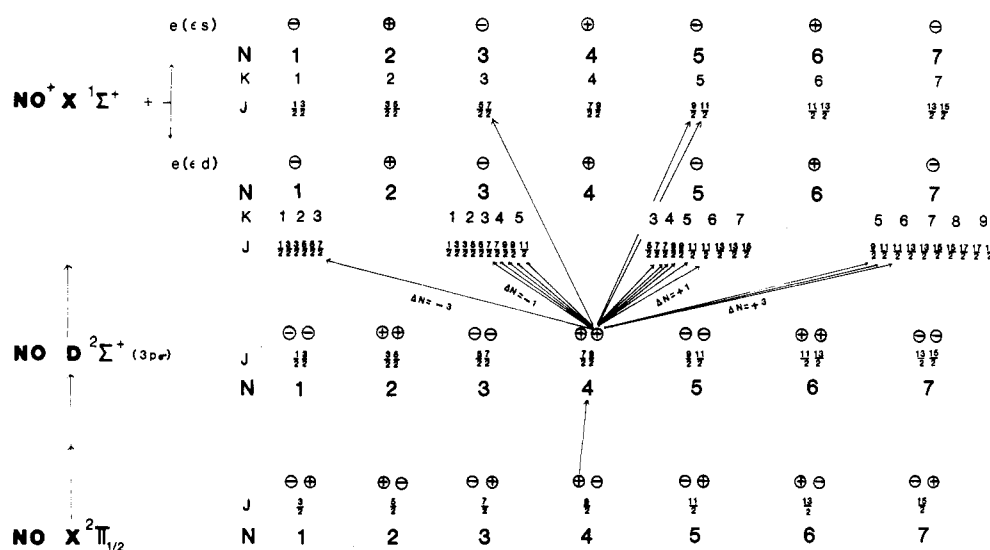


Figure 2. Allowed rotational transitions for a one-photon ionization from $J = 9/2$ of the D state.

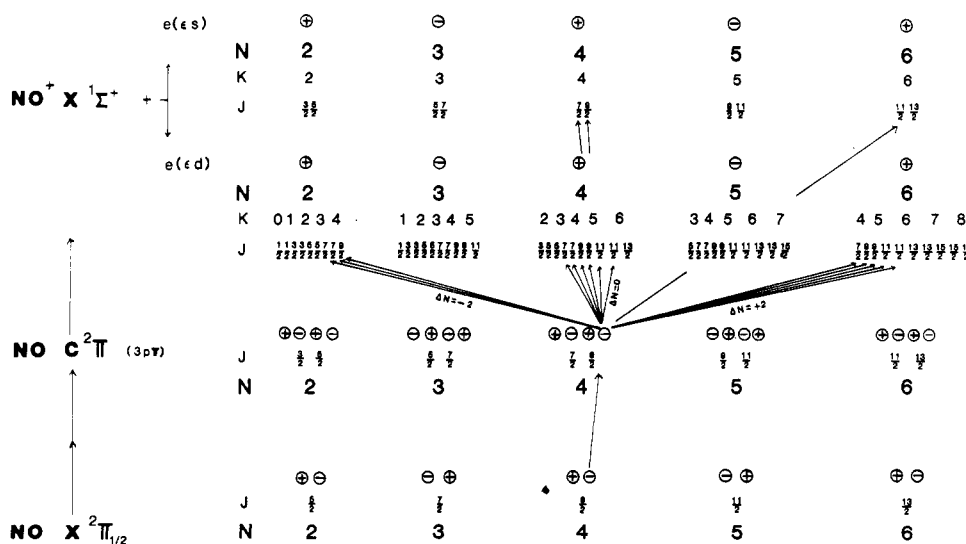


Figure 3. Allowed rotational transitions for a one-photon ionization from $J = 9/2$ ((-) parity) of the C state. For ionization from the (+) parity level of the same J , the propensity scheme would be exactly as shown in Figure 3 for the D state.

is resolved, the selection rules should be different for ionization out of the two different Λ -components, being either $\Delta N = 0, \pm 2$ or $\Delta N = \pm 1, \pm 3$.

As will be discussed, most of our experimental results are interpretable based on the simple model of Pratt et al. However, some discrepancies were found. These motivated us to perform

electronic structure calculations on the Rydberg states of NO which are described below.

Experimental Section

The time-of-flight (TOF) photoelectron spectrometer used in our experiments has been described elsewhere.⁸ The output from

a Quanta Ray Nd:YAG pumped dye laser with rhodamine 610 (for experiments on the D state) or Kiton Red 620 (for experiments on the C state) was frequency mixed with the fundamental of the YAG (1.06 μm) in a Quanta Ray WEX to yield wavelengths in the region 3750–3850 \AA appropriate for two-photon excitation of the two Rydberg states. An etalon was inserted into the YAG cavity in order to obtain a reduced bandwidth ($\sim 0.6 \text{ cm}^{-1}$) for the frequency-mixed output.

The 0–0 band profiles of the C–X and D–X transitions were obtained by monitoring the total photoelectron yield as a function of wavelength, as the laser was grating tuned. When specific rotational lines were tuned to record photoelectron spectra, the line width of the frequency-mixed UV was further reduced to $\sim 0.2 \text{ cm}^{-1}$ by inserting an air-spaced etalon in the dye laser cavity. The laser wavelength was then varied by pressure-scanning with nitrogen.

Photoelectron spectra were obtained by exciting moderately high rotational levels in the Rydberg states so that the ion rotational levels accessed in the photoionization process were separated enough to be resolved by our spectrometer. The plane of polarization of the laser was either parallel or perpendicular to the electron flight direction as noted. It was rotated with a Babinet-Soleil compensator. About 80 (C state) to 350 μJ (D state) per pulse were used to obtain photoelectron spectra. (These energies are higher than the 2 μJ per pulse used in our previous experiments involving the A state of NO.¹⁹ This is because excitation of the C and D states involves a two-photon process, whereas the A state can be conveniently reached with one photon.) At these intensities the count rates in our photoelectron experiments were on the order of 0.1 electron per laser shot. We employed such low count rates to prevent peak broadening due to space charge effects.⁵ It is also interesting to note that higher light intensities were required for the D state than the C state.

An effusive beam of NO (Matheson, Grade CP) streamed into the ionization chamber where a pressure of 3×10^{-5} Torr was maintained. Photoelectrons generated by laser ionization were detected with two Varian-8900 microchannel plates in tandem. The resulting signal was amplified and digitized with a Biomation 6500 waveform recorder and LeCroy 2228A time to digital converter (TDC), with time resolutions of 2 ns/channel and 250 ps/channel, respectively. Photoelectron spectra displayed in this paper were obtained with the TDC.

Theoretical Calculations

For the purpose of understanding, in detail, the Rydberg states of NO, it is necessary to use a very large basis of diffuse functions. At the same time an accurate description of the charge distribution in NO^+ requires a large basis of valence functions. We have compromised and used a fairly tight contraction of a large atomic set with an uncontracted Rydberg basis. Thus our atomic basis consisted of five s, four p, and two d type contracted Gaussians. A (6s, 5p, 4d, 2f) Rydberg set with smaller exponents was placed at the center of mass (we also tried the center of charge with nearly identical results). This basis gave an energy of -128.9649 hartrees at the bond length of NO^+ of 2.008 799 bohrs. By comparison, numerical Hartree Fock gives -128.9778 .

Because NO^+ is a closed-shell ion, the virtual orbitals of NO^+ form a natural basis for describing the Rydberg states of NO. By Koopmans' theorem, the negatives of the virtual orbital energies are approximately the ionization potentials of the Rydberg states. In fact, only small relaxation and correlation corrections are expected. The error in this estimate of the IP is only 7.5% for the 3s state.

In Table I we give the calculated energy of each orbital. We also give the total energy of each Rydberg state as derived from a MRSD-CI where the reference configurations were Slater determinants with one electron in a virtual orbital of NO^+ . It should be noted that with this basis there is no mixing between the reference configurations until higher excitations are included.

Because NO^+ is "almost" symmetrical, one would expect that the higher Rydberg orbitals would show only small mixing between hydrogen components of different parity. This expectation is borne

TABLE I: Calculated Energies (Hartree Units)

	orbital E	CI state E^a	exptl term
$2p\pi \text{ } X^2\Pi$	-0.279 96		-0.340
$3s\sigma \text{ } A^2\Sigma^+$	-0.129 47	-129.096 59	-0.140
$3p\pi \text{ } C^2\Pi$	-0.094 87		-0.103
$3p\sigma \text{ } D^2\Sigma^+$	-0.091 69	-129.058 95	-0.098
$4s\sigma/3d\sigma \text{ } E^2\Sigma^+$	-0.059 70	-129.025 04	-0.064
$3d\pi \text{ } H^2\Pi$	-0.053 03		-0.056
$3d\sigma/4s\sigma \text{ } H^2\Sigma^+$	-0.052 90	-129.018 40	-0.056
$4p\sigma \text{ } M^2\Sigma^+$	-0.043 53	-129.008 92	-0.047
$5s\sigma/4d\sigma \text{ } S^2\Sigma^+$	-0.032 68	-128.997 77	-0.035
$4f\sigma \text{ } ^2\Sigma^+$	-0.030 79		-0.032

^a CI calculations were only done for Σ states.

TABLE II: Orbital Mulliken Population Analysis and Rydberg "s" Coefficients in Rydberg Orbitals

A. Mulliken Population Analysis					
	s	p	d	N(sp <i>d</i>)	O(sp <i>d</i>)
3 <i>sσ</i>	0.976	0.001	0.019	0.008	0.000
3 <i>pσ</i>	0.005	0.988	0.004	0.001	0.000
4 <i>sσ</i> /3 <i>dσ</i>	0.581	0.009	0.407	0.005	-0.002
3 <i>dσ</i> /4 <i>sσ</i>	0.414	0.000	0.585	0.001	0.000
4 <i>pσ</i>	0.007	0.987	0.005	0.002	0.000
5 <i>s</i> /4 <i>dσ</i>	0.486	0.012	0.504	0.003	-0.001

B. Rydberg "s" Coefficients						
	3 <i>sσ</i>	3 <i>pσ</i>	4 <i>s</i> /3 <i>dσ</i>	3 <i>d</i> /4 <i>sσ</i>	4 <i>pσ</i>	5 <i>s</i> /4 <i>dσ</i>
Rs1 ^a	-0.157	0.058	0.037	0.206	-0.047	-0.038
Rs2	-0.832	0.045	-0.870	-0.666	-0.037	0.817
Rs3	0.415	-0.096	0.544	0.016	0.166	-1.302
Rs4	-0.082	0.008	0.623	0.834	-0.145	0.462
Rs5	0.034	-0.004	-0.143	-0.169	0.008	0.621
Rs6	-0.010	0.001	0.039	0.046	-0.003	-0.122

^a Gaussian s basis functions on center of mass with exponents 0.1, 0.031 623, 0.01, 0.003 162 3, 0.001, and 0.000 816 23.

out in the SCF calculation as will be seen below. The CI results indicate that this trend persists and the strongest mixing is between configurations of the same parity. Even this mixing is weak, however, so that the Koopmans' states derived with the SCF orbitals of NO^+ have coefficients exceeding 0.99 in the final CI wavefunctions.

A Mulliken population analysis of the Rydberg orbitals is given in Table IIA. Contributions from s, p, and d orbitals located at the center of mass of the N and O nuclei are indicated. It is evident that there is little mixing between states of different hydrogenic parity. However, because of the large quantum defect of the ns states, they are accidentally degenerate with the $(n-1)$ d states. This leads to very large s–d mixing for $n > 3$ as implied by our labels for the E, H, and S states in Table I. However, the $3s\sigma$ and $3p\sigma$ molecular orbitals excited in our experiment have almost pure s and p character, respectively. These results are in basic agreement with recent calculations of Kaufman et al.²¹ They obtained an SCF energy of $-128.925 445$ hartrees, indicating that our valence basis set is better than theirs but their Rydberg basis is much more extensive than ours.

One trend apparent in Table IIA is somewhat counterintuitive. One might have expected that as the principal quantum number n increases, the excited state orbitals would become more hydrogenic since the core should look more like a point charge. More precisely, the s–p and p–d interaction matrix elements should decrease as n^{-4} while the energy difference between two Rydberg states of the same n but different l should decrease as n^{-3} . Consequently, the "s" character in a "p" orbital, which is proportional to the square of the ratio of these terms, should decrease as n^{-2} . However, for Table IIA it is evident that s–p mixing actually seems to increase with increasing principal quantum number. For the low n values considered here, the source of this apparent dichotomy is s–d mixing. As a result of it, np states fall midway in energy between the $(n+1)s/nd$ and $(n-1)d/ns$ levels

TABLE III: Transition Moments (ea_0)

	3p	4s/3d	3d/4s	4p	5s/4d
Koopmans' Theorem					
3s	3.278	0.256	0.055	0.004	0.099
3p		4.922	1.628	0.335	0.624
4s/3d			0.038	7.269	0.419
3d/4s				1.909	0.443
4p					11.302
Configuration Interaction					
3s	3.116	0.250	0.044	0.109	0.094
3p		4.761	1.375	0.324	0.599
4s/3d			0.009	7.195	0.460
3d/4s				2.150	0.460
4p					11.105

TABLE IV: Analysis of SCF Transition Moments^a

3s → 3p	3.7 (s → p)	-0.2 (d → p)	
3s → 4s	0.3 (s → p)		
3s → 5s	0.1 (s → p)		
3p → 4s	2.3 (p → s)	2.6 (p → d)	
3p → 3d	-1.4 (p → s)	3.1 (p → d)	
3p → 4p	0.2 (s → p)		
3p → 5s	0.5 (p → s)	0.1 (p → d)	
4s → 4p	5.4 (s → p)	1.9 (d → p)	
4s → 5s	0.4 (s → p)		
3d → 4p	5.5 (s → p)	-3.6 (d → p)	
3d → 5s	0.5 (s → p)	-0.2 (d → p)	0.2 (d → f)
4p → 5s	5.2 (p → s)	6.2 (p → d)	

^a Each line gives the main contributions to the total transition moment grouped by angular momentum components in the orbitals involved. There were no significant contributions from the atom-centered basis functions.

and consequently mix with both of these. As Table IIB shows, the coefficients of the "A" Rydberg-type basis functions in the "p" orbitals are not in the same ratio as they are in any of the "s" orbitals. For example the "s" component of 4pσ cannot be identified as simply "4s" or "5s".

These calculations can help us understand why transitions between certain Rydberg states, which are expected to be highly forbidden in a hydrogenic model, have actually been experimentally observed. For example, Cheung et al.²² and Anezaki et al.²³ have observed Rydberg-Rydberg transitions from 3sσ A(2Σ⁺) to "ns" and "nf" states, in addition to the "np" series. They rationalized their observations as being due to orbital mixing in the A state. In an effort to clarify this, transition moment calculations were performed. Table III gives computed moments for several transitions at both the Koopmans' theorem and CI level. As expected from the small mixing observed in the CI, these two results are very similar. In almost all cases it suffices to analyze the SCF result. One exception to this is the 3s → 4p transition. The small mixing of the 3p configuration into the 4p state causes the 3s → 4p CI transition moment to be much larger than the corresponding SCF value.

The most obvious feature of Table III is that the strongly allowed (s ↔ p, p ↔ d, Δn = 0) transitions are predicted to be much more intense than the nominally forbidden ones. The typical intensity ratio, as judged by the squares of the transition moments, is about 100:1. Unfortunately, in spite of all the experimental work that has been done on Rydberg-to-Rydberg transitions, no measurements of these relative intensities are available.

Table IV is the result of partitioning the SCF transition moment integral into contributions from the same categories of basis functions as were used in the population analysis. Only contributions greater than 0.1 are shown. The 3s → 4p transition appears to be somewhat anomalous since the single s → p contribution in Table IV is much larger than the total transition moment indicated in Table III. This results from cancellation

by d → p and several other small terms. The most important conclusion to be extracted is that for each transition considered, it is the mixing in the *higher* state that causes the hydrogenic selection rules to be violated. This contrasts with previous thinking about Rydberg-Rydberg transitions and will be relevant to discussions of our laser photoelectron spectra below.

Results and Discussion

In all our experiments on the A, C, and D states we excited specific rotational levels in $v = 0$ vibrational levels in order to record our photoelectron spectra. Since the Rydberg states have potential curves almost parallel to that of the ion, Franck-Condon factors favor Δv = 0 ionization transitions.²⁴ Indeed in all three cases we have observed dominant photoelectron peaks corresponding to transitions to the $v = 0$ level of the ion, with extremely weak $v = 1$ signals. Earlier studies on NO^{10,11} have observed non-Franck-Condon peaks that have been attributed to autoionization. In these photoelectron experiments, we have only studied the Franck-Condon allowed Δv = 0 transitions and recorded spectra corresponding to production of ions in their ground vibrational state.

A State. As mentioned earlier, we have previously published a rotationally resolved photoelectron spectrum by exciting the R(21.5) line of the X → A transition.¹⁹ With the incident light polarized parallel to the flight tube, we observed a ΔN = 0, ±2 propensity. Calculations of the rotational branching ratios by Dixit et al. are in qualitative agreement with our results.²⁵ However, in addition to the observed propensities, they also predicted nonzero branching ratios for ΔN = ±1 transitions, arising from electrons scattered into s and d wave channels. In the ionization of the A state an electron is ejected from a 3sσ molecular orbital. Our calculations described in the previous section have shown that this electron has almost no p or d character. In a united atom picture only p wave channels should be allowed for the outgoing electron due to the Δl = ±1 selection rule. However, according to Dixit et al., the noncentral field of the NO⁺ ion can induce ΔN = ±1 channels in the ionization process. In our experiments we did not see any evidence of the ΔN = ±1 peaks, but it was possible that these could have been buried under the strong signal due to the ΔN = 0, ±2 peaks. However, with the polarization of the laser perpendicular to the flight tube, the p wave channel should be discriminated against, and the weak s or d wave channel leading to ΔN = ±1 peaks might become evident. We therefore repeated our earlier experiment on the A state, pumping the same transition but with light polarized perpendicular to the flight tube. The overall detected electron signal was greatly reduced. However, as is apparent in Figure 4 the dominant structure is still due to the ΔN = 0, ±2 peaks and we could not observe any peaks associated with odd changes in N.

C State. Monitoring the total photoelectron signal as a function of wavelength in the region of the 0-0 band of the X-X transition yielded a band profile similar to that published by Sirkin and Haas.¹⁸ The rotational line positions were calculated with the high-resolution work of Miescher and Lagerquist¹⁴ on the C state together with the term values for the rotational levels of the X state published by Kristiansen.²⁶ The spectrum is dominated by Q branches as is expected for a two-photon Π → Π transition.^{27,28} The A-doubling in the C state is quite large (~3 cm⁻¹ near J = 13.5) and is resolved in our spectrum. In contrast the spin splitting for the corresponding N is only about 0.3 cm⁻¹. This is of no serious consequence, since the strength of the Q branch transitions relative to the P and R branches enables us to preferentially populate only one of the spin components, F₁ or F₂. Furthermore,

(24) (a) Herzberg, G. *Spectra of Diatomic Molecules*; Von Nostrand: New York, 1950. (b) Gilmore, F. J. *Quant. Spectrosc. Radiat. Transfer* **1965**, *5*, 369.

(25) Dixit, S. N.; Lynch, D. L.; McKoy, V.; Huo, W. M. *Phys. Rev. A* **1985**, *32*, 1267.

(26) Kristiansen, P. J. *Mol. Spectrosc.* **1977**, *66*, 177.

(27) Bray, R. G.; Hochstrasser, R. M. *Mol. Phys.* **1976**, *31*, 1199.

(28) Freedman, P. A. *Can. J. Phys.* **1977**, *55*, 1388.

(22) Cheung, W. Y.; Chupka, W. A.; Colson, S. D.; Gauyacq, D.; Avouris, P.; Wynne, J. J. *J. Chem. Phys.* **1983**, *78*, 3625.

(23) Cheung, W. Y.; Colson, S. D. *Advances in Laser Spectroscopy*; Wiley: London, 1983; Vol. 2, p 73.

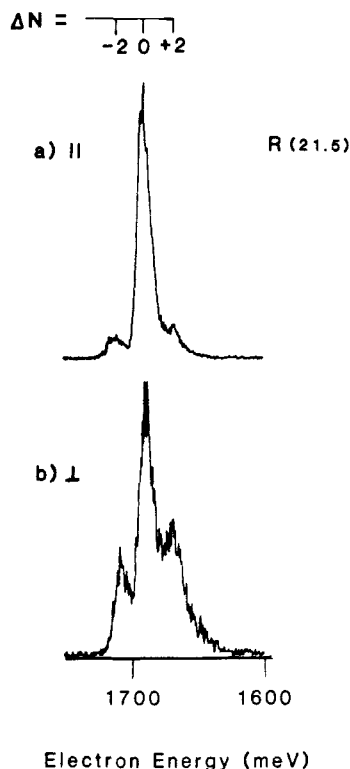


Figure 4. Photoelectron spectra with laser tuned to the R(21.5) line of 0-0 band of the $A \leftarrow X$ transition with (a) laser polarized parallel to the electron flight direction and (b) laser polarized perpendicular to the electron flight direction.

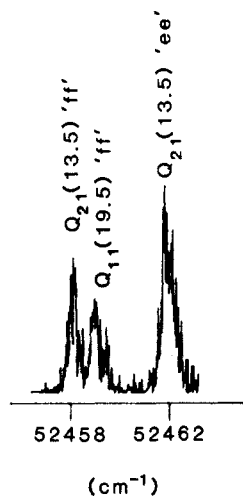


Figure 5. Pressure scan of a portion of the 0-0 band of the $C \leftarrow X$ transition near the region of the $Q_{21}(13.5)$ line.

when Λ -doubling and spin splitting are taken into consideration the F_1 and F_2 components that group together have the same parity and therefore do not affect the predicted rotational selection rules.

Figure 5 shows the pressure scan of the region near 3811 Å, spanning the two Λ -doubling components of the $Q_{21}(13.5)$ lines. From this it is evident that individual rotational levels can be selectively excited. The $Q_{21}(13.5)$ "ee" line is somewhat stronger than the $Q_{21}(13.5)$ "ff" line. This is consistent with the observations of Rottke and Zacharias that the "e" component in the $^2\Pi_z$ ($\equiv F_2$ for high J) showed consistently greater intensity in both fluorescence and ionization.²⁹ Here the "e" and "f" refer to the nomenclature introduced by Kopp and Hougen,³⁰ where, levels with parity $+(-1)^{J-(1/2)}$ are "e" levels, and levels with parity $-(-1)^{J-(1/2)}$ are "f" levels.

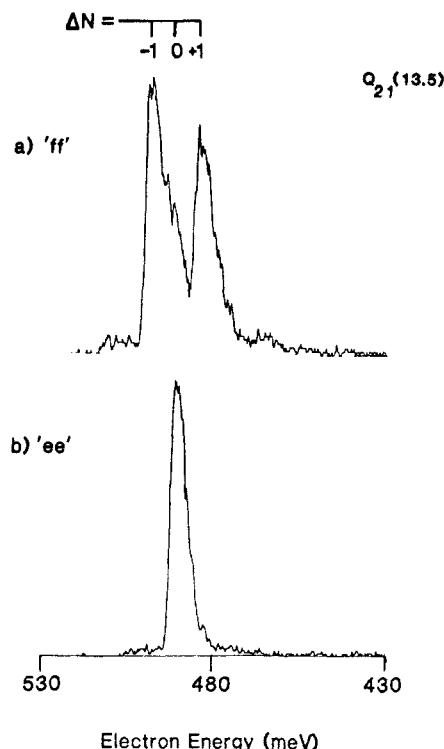


Figure 6. Photoelectron spectra (a) with the laser tuned to the $Q_{21}(13.5)$ "ff" line and (b) with the laser tuned to the $Q_{21}(13.5)$ "ee" line.

As mentioned earlier, if Λ -doubling is resolved and each component for a given J is excited separately, the propensity for rotational transitions in the ionization process differs for the two components. For example when ionizing from the level of (+) parity ("f" level) of $J = 13.5$ ($N = 14$) of the C state, a propensity of $\Delta N = \pm 1, \pm 3$ is expected, whereas ionization from the level of (-) parity ("e" level) of the same J is expected to yield a $\Delta N = 0, \pm 2$ propensity.

Figure 6 shows photoelectron spectra obtained by tuning the laser to the $Q_{21}(13.5)$ lines, thus exciting the $J = 13.5$ (F_2 component of $N = 14$) level in the C state. At these high J levels, complications due to predissociation are avoided, since for levels $N \geq 6$ ($v = 0$) no sign of predissociation has been observed.³¹ In Figure 6a the laser wavelength is tuned to excite a level of (+) parity (f level). Large $\Delta N = \pm 1$ and small $\Delta N = \pm 3$ peaks are observed. The observed spacings between the peaks in the spectrum agree to within 1 meV with the calculated spacings between the relevant J (or N) levels of the ion obtained by using the rotational constants for the X state of the ion.³² In Figure 6b, the (-) parity (e level) of the same J was excited by tuning to the second component of the $Q_{12}(13.5)$ transition. A strong $\Delta N = 0$ peak was observed in this case.

We next investigated the polarization dependence of the photoelectron spectra. Figure 7 compares photoelectron spectra obtained with the light polarized parallel (Figure 7a) and perpendicular (Figure 7b) to the electron flight direction for the transition $Q_{12}(13.5)$ when the "e" level was pumped. The relative intensities of the $\Delta N = 0$ and $\Delta N = \pm 2$ peaks are seen to be polarization dependent. While the $\Delta N = 0$ peak was largest in both cases, the $\Delta N = \pm 2$ peaks that are hardly discernible when the laser is polarized parallel (Figure 7a) stand out very clearly when the laser polarization is rotated by 90°. Similar results were obtained when photoelectron spectra were obtained by exciting different components of the $Q_{12}(12.5)$ lines. Theoretical calculations on the relative intensities of the photoelectron peaks are needed in order to quantitatively explain these results.

Müller-Dethlefs et al., using photoionization resonance spectroscopy, have also obtained rotational selection rules for ionization

(29) Rottke, H.; Zacharias, H. *J. Chem. Phys.* **1985**, *83*, 4831.

(30) Kopp, I.; Hougen, J. T. *Can. J. Phys.* **1967**, *45*, 2581.

(31) Miescher, E. *J. Mol. Spectrosc.* **1974**, *53*, 302.

(32) Huber, K. P.; Herzberg, G. *Constants of Diatomic Molecules*; Van Nostrand Reinhold: New York, 1979.

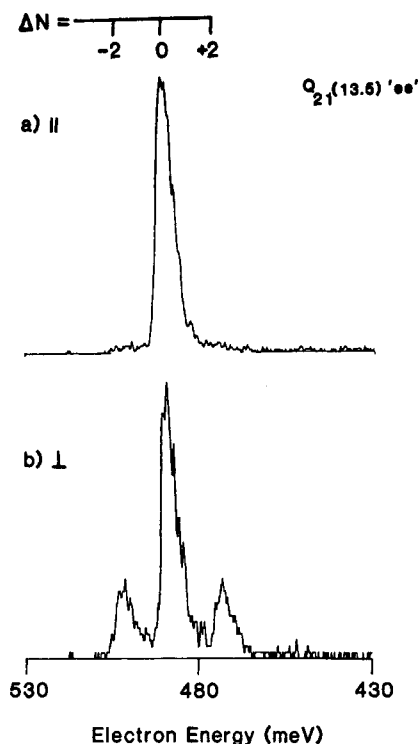


Figure 7. Photoelectron spectra with the laser tuned to the $Q_{21}(13.5)$ "ee" line and (a) polarized parallel to the electron flight direction and (b) laser polarized perpendicular to the electron flight direction.

from the C state.³³ They ionized from the $T_y(1/2)$ level and observed $\Delta J = \pm 1/2, \pm 3/2$ with small contributions from $\Delta J = \pm 5/2$. However, since they were exciting low J levels, the Λ -doubling in the C state was not resolved and the dependence of the rotational selection rules on the parity of the pumped level was not studied. When our selection rules on ΔN are translated to selection rules on ΔJ , our results are in agreement with theirs provided that Λ -doubling is not taken into account. At first sight this agreement may appear somewhat surprising, since the low J levels pumped by Müller-Dethlefs et al. are perturbed by the B state,³¹ whereas the higher J levels accessed in our experiments are not. However, since the ionization cross section of the B state is about 2–3 orders of magnitude smaller than that of the C state,²⁹ their photoionization spectrum was probably dominated by C-state characteristics.

D State. Monitoring the total photoelectron yield as a function of wavelength in the region of the 0–0 band of the D–X transition yielded a spectrum that agreed well with that obtained by Asscher and Haas.¹⁷ The rotational line assignments were calculated with the constants for the D and X states of NO.³²

A pressure scan of the region near 3739 Å, spanning the $S_{12}(11.5)$ and $(S_{11} + R_{21})(15.5)$ lines, is shown in Figure 8. After this was recorded the laser was tuned to the wavelength of the $S_{11} + R_{21}(15.5)$ line, thereby exciting the $N = 17$ level in the D state. The photoelectron spectrum obtained at this wavelength, with the light polarized parallel to the electron flight direction (horizontal polarization), is shown in Figure 8a. Peaks corresponding to $\Delta N = 0, \pm 1, \pm 3$ transitions are observed.

The $\Delta N = 0$ peak was unexpected and we have considered possible explanations for its appearance. If the Rydberg electron in the D state were not adequately describable as a pure "3p σ " electron but in fact has some "s" character, then the ejected electron wave function would be expected to have some "p" character. According to the selection rule scheme of Figure 3, this would account for the $\Delta N = 0$ peak. However, as can be seen from Table II, our calculations indicate that the Rydberg electron excited in the D state contains almost no s or d character.

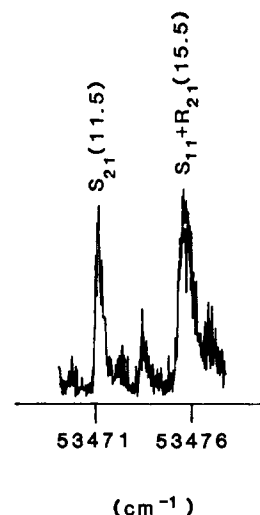


Figure 8. Pressure scan of the portion of the 0–0 band of the D ← X transition near the region of the $S_{21}(11.5)$ line.

Therefore it is more likely that the mixed character is in the continuum wavefunction that describes the ejected electron. This is the hypothesis proposed by Dixit et al. in their work on NO A state ionization.²⁵ Although we could not directly test this, we were able to investigate the angular dependence of the anomalous $\Delta N = 0$ peak in the D-state spectrum. We hypothesized that the $\Delta N = 0$ peak arises from p wave contributions to the continuum orbital, whereas the $\Delta N = \pm 1, \pm 3$ peaks arise from the predominantly s and d wave contributions expected from ionizing a 3p σ Rydberg electron. If this interpretation is correct, then the two sets of peaks should exhibit different angular dependences. An outgoing p wave (leading to the $\Delta N = 0$ peak) would be expected to show "cos² θ " type dependence.³⁴ Hence it should have a maximum probability along the polarization axis of the laser and zero probability perpendicular to it. Outgoing s and d waves (leading to the $\Delta N = \pm 1, \pm 3$ peaks), being somewhat more isotropic, are detectable both parallel and perpendicular to the polarization axis of the laser. This implies that with the laser polarized perpendicular to the electron flight direction to the detector the $\Delta N = 0$ peak should have zero intensity but the $\Delta N = \pm 1, \pm 3$ peaks should still appear, though, possibly, with different intensities.

To check the above hypothesis, a photoelectron spectrum was obtained by exciting the same transition as in Figure 9a but with the laser polarized perpendicular to the electron flight direction. The total photoelectron signal detected in this case was lower by approximately a factor of 3 compared with the intensity obtained with the laser polarized parallel to the flight tube direction. Due to the low photoelectron count rates in our experiments, each experiment was signal averaged over as many as 300 000 laser shots. Figure 9b shows the photoelectron spectrum obtained by pumping the $S_{11} + R_{21}(15.5)$ line with the laser polarized vertically. The $\Delta N = 0$ peak is clearly absent in the vertically polarized spectrum. This strongly suggests that it is the p wave contribution to the continuum orbital that leads to the appearance of this $\Delta N = 0$ peak. Since our detector's solid angle of acceptance is very small, our apparatus actually discriminates in favor of detecting properly oriented anisotropic p waves relative to the more isotropic angular distribution obtained by ejecting an electron from a p orbital. Furthermore, the A- and C-state experiments indicate that whenever a $\Delta N = 0, \pm 2$ propensity is allowed most of the intensity tends to accumulate in just the $\Delta N = 0$ channel, yielding a single intense peak. These factors qualitatively imply that even a small amount of "p" character in the continuum wavefunction may explain the rather substantial $\Delta N = 0$ peak in the Figure 9a spectrum. Theoretical calculations on the continuum orbitals are clearly needed before the method can contribute to improving

(33) Müller-Dethlefs, K.; Sander, M.; Schlag, E. W. *Chem. Phys. Lett.* **1984**, *112*, 291.

(34) Rabalais, J. W. *Principles of Ultraviolet Photoelectron Spectroscopy*; Wiley: New York, 1977.

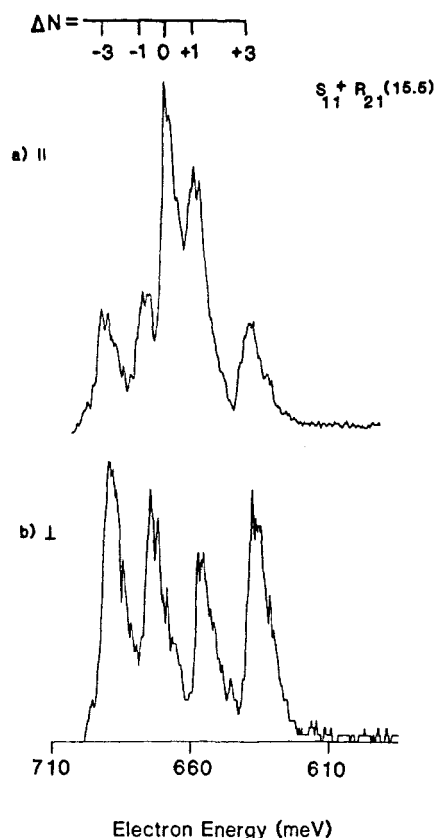


Figure 9. Photoelectron spectra with the laser tuned to the $S_{11} + R_{21}$ (15.5) line of the $D \leftarrow X$ transition with (a) laser polarized parallel to the electron flight direction and (b) laser polarized perpendicular to the electron flight direction.

our understanding of molecular excited state wavefunctions. Note that the present model is consistent with the conclusion drawn from our calculations that mixing among higher Rydberg states occurs to a greater extent than mixing among lower Rydberg states.

Figure 10 depicts photoelectron spectra obtained with horizontally and vertically polarized light tuned to the S_{12} (11.5) transition, thus exciting the $N = 14$ level in the D state. We again observed only a $\Delta N = \pm 1, \pm 3$ propensity in the vertically polarized spectrum, whereas the horizontally polarized laser yielded a $\Delta N = 0$ propensity also. The fact that $\Delta N = 0$ peaks appear in both Figures 9a and 10a and are absent in both Figures 9b and 10b suggests that it is highly unlikely that they result from fortuitous overlap between unresolved $D \leftarrow X$ spectral lines.

Conclusions

The propensity for rotational transitions in photoionization processes agrees well both with the theoretical predictions of Bonham¹² and the model used by Pratt et al.⁹ In the case of ionization from the $A^2\Sigma^+$ and $C^2\Pi$ states, experiments yielded exactly what was predicted. Two different parity components of

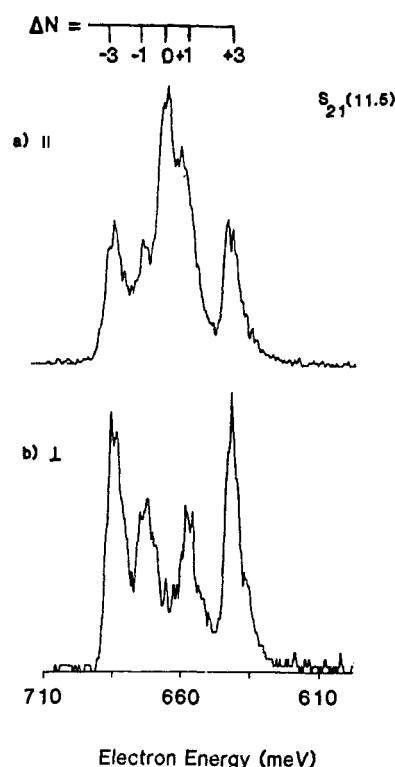


Figure 10. Photoelectron spectra with the laser tuned to the S_{21} (11.5) line of the $D \leftarrow X$ transition with (a) laser polarized parallel to the electron flight direction and (b) laser polarized perpendicular to the electron flight direction.

a given J level of the C state were individually excited and different propensities were observed as expected. In the case of the $D^2\Sigma^+$ state we observed a strong $\Delta N = 0$ peak even though only odd changes in N were predicted. We believe that the $\Delta N = 0$ peak arises through orbital mixing in the continuum. This speculation is supported by our angular distribution experiments in which the $\Delta N = 0$ peak completely vanished when the photoelectron spectrum was recorded with the laser light polarized perpendicular to the electron flight direction.

The study of rotational propensities, by yielding information on the partial waves of the ejected electron, can in principle provide a description of the molecular orbital from which the electron is ionized. Such studies should be very useful in probing orbital mixing since the polarization dependence of photoelectron spectra can be used to gain information on the nature of the interaction.

Acknowledgment. This work has been supported by the National Science Foundation under Grant NSF-CHE-83-14536 and by the Office of Research and Development, Environmental Protection Agency, under Grant R812830-01-0. We thank Prof. F. Franz for the loan of a Babinet-Soleil compensator and are very grateful to Dr. P. Dehmer for helpful discussions.

Registry No. NO, 10102-43-9.